Moesin and its activating kinase Slik are required for cortical stability and microtubule organization in mitotic cells

Sébastien Carreno,[1] Ilektra Kouranti,[2] Edith Szafer Glusman,[3] Margaret T. Fuller,[3] Arnaud Echard,[2] and François Payre[1]

[1]Centre de Biologie du Développement, Université Toulouse III/Centre National de la Recherche Scientifique, Unité Mixte de Recherche 5547, 31062 Toulouse Cedex 09, France
[2]Institut Curie/Centre National de la Recherche Scientifique, Unité Mixte de Recherche 144, 75248 Paris Cedex 05, France
[3]Department of Developmental Biology and Genetics, School of Medicine, Stanford University, Stanford, CA 94305

Cell division requires cell shape changes involving the localized reorganization of cortical actin, which must be tightly linked with chromosome segregation operated by the mitotic spindle. How this multistep process is coordinated remains poorly understood. In this study, we show that the actin/membrane linker moesin, the single ERM (ezrin, radixin, and moesin) protein in *Drosophila melanogaster*, is required to maintain cortical stability during mitosis. Mitosis onset is characterized by a burst of moesin activation mediated by a Slik kinase–dependent phosphorylation. Activated moesin homogenously localizes at the cortex in prometaphase and is progressively restricted at the equator in later stages. Lack of moesin or inhibition of its activation destabilized the cortex throughout mitosis, resulting in severe cortical deformations and abnormal distribution of actomyosin regulators. Inhibiting moesin activation also impaired microtubule organization and precluded stable positioning of the mitotic spindle. We propose that the spatiotemporal control of moesin activation at the mitotic cortex provides localized cues to coordinate cortical contractility and microtubule interactions during cell division.

Introduction

A central feature of animal cell division is the coordination between actin-mediated cell shape transformations and microtubule spindle dynamics. At mitosis entry, RhoA-dependent reorganization of actin at the plasma membrane induces cortical stiffness and rounding of the cell (Matzke et al., 2001; Maddox and Burridge, 2003). Subsequently, anisotropic actin distribution leads to polar relaxation and equatorial contraction, which contributes to anaphase cell elongation (Hickson et al., 2006) and drives the early stages of cytokinesis (Glotzer, 2005; Eggert et al., 2006). At cytokinesis onset, a subset of spindle microtubules becomes stabilized at the equatorial cortex (Canman et al., 2003; Strickland et al., 2005a,b) and locally stimulates RhoA-dependent actomyosin contractions (Bement et al., 2005; Glotzer, 2005; Eggert et al., 2006). Conversely, astral microtubules remain more dynamic in the polar regions undergoing cortical relaxation (Canman et al., 2003). A key unresolved question is how the localized assembly and contraction of cortical actomyosin that shape the dividing cell are regulated and coupled to the microtubule spindle throughout mitosis.

ERM (ezrin, radixin, and moesin) proteins, which link actin with membrane proteins in a signal-dependent manner, participate in the regulation of cortical cohesion in interphase (Bretscher et al., 2002; Polesello et al., 2002; Charras et al., 2005; Hughes and Fehon, 2007). During mitosis, ERM proteins have long been known to be activated at the cleavage furrow (Sato et al., 1991), but their potential role in cell division was presumably hampered by functional redundancy between ezrin, radixin, and moesin in vertebrates. Studies in *Drosophila melanogaster*, which encodes a unique ERM gene (*dmoesin* or *moesin*), have revealed roles for ERM proteins in cell polarity (Polesello et al., 2002; Pilot et al., 2006), epithelial integrity (Speck et al., 2003; Hipfner et al., 2004) and light response (Chorna-Ornan et al., 2005). Here, we show that the activation of moesin is critical to maintain cortical stability, spindle organization, and proper spindle position in mitotic cells.

A. Echard and F. Payre contributed equally to this paper.
Correspondence to Sébastien Carreno: carreno@cict.fr
S. Carreno's present address is Institute for Research in Immunology and Cancer, Université de Montréal, Montréal, Québec H2W 1R7, Canada.

Abbreviations used in this paper: dsRNA, double-stranded RNA; F-actin, filamentous actin; p-moesin, phosphorylated moesin.

The online version of this article contains supplemental material.

The Journal of Cell Biology, Vol. 180, No. 4, February 25, 2008 739–746
http://www.jcb.org/cgi/doi/10.1083/jcb.200709161

Results and discussion

Moesin is required for cortical stability during mitosis

We noticed that reduction of *moesin* activity led to a low proportion of cytokinesis defects in vivo, suggesting a putative role of moesin in mitosis (Fig. S1, available at http://www.jcb.org/cgi/content/full/jcb.200709161/DC1). Because available *moesin* alleles may retain significant moesin levels (Jankovics et al., 2002; Polesello et al., 2002; Karagiosis and Ready, 2004; Pilot et al., 2006), we used the depletion of moesin by double-stranded RNA (dsRNA) in S2 cultured cells to further investigate moesin function during cell division. Although previous large-scale screens failed to reveal a role of moesin in mitotic cells (Echard et al., 2004; Eggert et al., 2004; Bjorklund et al., 2006), we found that the dsRNA treatments used in these studies did not significantly reduce moesin levels. We obtained conditions of efficient moesin depletion (Fig. S1) and observed that moesin fulfills important roles in cell division.

Besides a low rate of cytokinesis failure, the main defects resulting from efficient moesin inhibition in S2 cells were observed in earlier mitotic stages. First, we noticed an increased proportion of cells in metaphase compared with the other stages of cell division, showing that moesin depletion caused a delay in anaphase onset (Fig. 1 A). Second, live cell imaging revealed a role of moesin in cell shape changes throughout cell division. The volume of moesin-depleted cells in metaphase was significantly increased when compared with controls (Fig. 1 and Fig. S2 A, available at http://www.jcb.org/cgi/content/full/jcb.200709161/DC1). Furthermore, as early as prophase and until telophase, moesin-depleted cells displayed large and transient cytoplasmic bulges that deformed the mitotic cortex (Fig. 1, B and C; and see Fig. 4 B). These results suggest that moesin depletion impairs cortical integrity and rigidity. Interestingly, ezrin was shown to be critical for the resorption of short-lived blebs induced by the alteration of cortical tension in mammalian cells (Charras et al., 2005). Consistent with a role of moesin in the regulation of cortical contractility during mitosis, localization of contractile factors at the cortex was abnormal in dividing moesin-depleted cells. Unlike wild-type conditions, filamentous actin (F-actin) and myosin II were distributed irregularly, with an accumulation at cortical deformations in pro/metaphase, and were not properly restricted at the equator in ana/telophase of moesin-depleted cells (Fig. 1, C and D). Live analysis showed transient accumulation of the myosin regulatory light chain Sqh-GFP at ectopic sites of the metaphase cortex in moesin-depleted cells (Fig. 1 E and Videos 3 and 4). Previous work indicated that the increased cortical tension characteristic of early mitosis depends on the activity of the small GTPase Rho (Maddox and Burridge, 2003). We found that RhoA was abnormally localized in the absence of moesin. RhoA was unevenly distributed at the metaphase cortex and accumulated in the cortical deformations induced upon moesin depletion until later stages of cell division (Fig. 1 F). Consistently, the occurrence of cortical bulges was reduced (more than threefold) by the simultaneous depletion of RhoA along with moesin in S2 cells (Fig. S2). However, cells depleted for both RhoA and moesin still displayed highly abnormal mitosis, including increased cell volume and a high proportion of multinucleated cells (Fig. S2). Numerous studies have demonstrated a complex cross talk between Rho and ERM proteins (Bretscher et al., 2002) ranging from positive (Verdier et al., 2006) to antagonistic interactions (Speck et al., 2003; Hipfner et al., 2004) in different *Drosophila* tissues. Therefore, future studies will be required to further decipher the interactions that might exist between ERM proteins and the RhoA pathway during cell division. All together, our data show that moesin is required for the dynamic distribution of actomyosin contractility at the cortex to account for cell shape transformations during cell division.

The Slik kinase activates moesin and is required for cortical stability during mitosis

To efficiently link F-actin to the membrane, ERM proteins need to adopt an open conformation regulated by binding to phospholipids and phosphorylation of a conserved Thr residue (Coscoy et al., 2002). Antibodies specific for phosphorylated T559 (phosphorylated moesin [p-moesin]; Karagiosis and Ready, 2004) revealed that mitosis entry was characterized by a strong increase in moesin phosphorylation (Fig. 2 A). Levels of p-moesin remained elevated in all successive steps of cell division. The locations of p-moesin strictly paralleled, in time and space, sites of cortical contraction during division (Fig. 2 B). From prophase to metaphase, p-moesin was uniformly distributed at the mitotic cortex. In later stages, p-moesin became progressively restricted to the equator and accumulated at the cleavage furrow (Fig. 2 B).

To identify the kinase regulating moesin activation during cell division, we tested Thr/Ser kinases that were previously identified as essential for mitosis through genome-wide dsRNA screens (Bettencourt-Dias et al., 2004; Echard et al., 2004; Eggert et al., 2004; Bjorklund et al., 2006). For instance, we found that T559-moesin phosphorylation was unaffected by the depletion of Polo, Citron, or Rok kinases (unpublished data). In contrast, p-moesin was no longer detected at the cortex of dividing Slik-depleted cells (Fig. 2 D), showing that Slik/PLKK1 regulates moesin phosphorylation during mitosis, which is consistent with previous studies in interphase (Hipfner et al., 2004; Hughes and Fehon, 2006). Staining with the pan-moesin antibodies showed normal expression levels of moesin in Slik-depleted cells and some moesin signal associated with the cortex, likely representing non–p-moesin forms (Fig. 2 D). Importantly, using antibodies to detect the Slik kinase, we found that distribution of the Slik protein paralleled p-moesin localization throughout division in wild-type cells (Fig. 2 C). In addition, the inactivation of Slik affected mitosis in a manner remarkably similar to the loss of moesin function. First, cytokinesis defects were observed in Slik-depleted S2 cells and in Slik mutants in vivo (unpublished data). Second, cells depleted for Slik displayed an elongated metaphase, as deduced from the increased proportion of metaphase stages among mitotic cells (51.6 vs. 32.6% in controls). Third, as observed after moesin depletion, the absence of Slik significantly increased the volume of pro/metaphase cells (Fig. S2). Finally, Slik inactivation induced

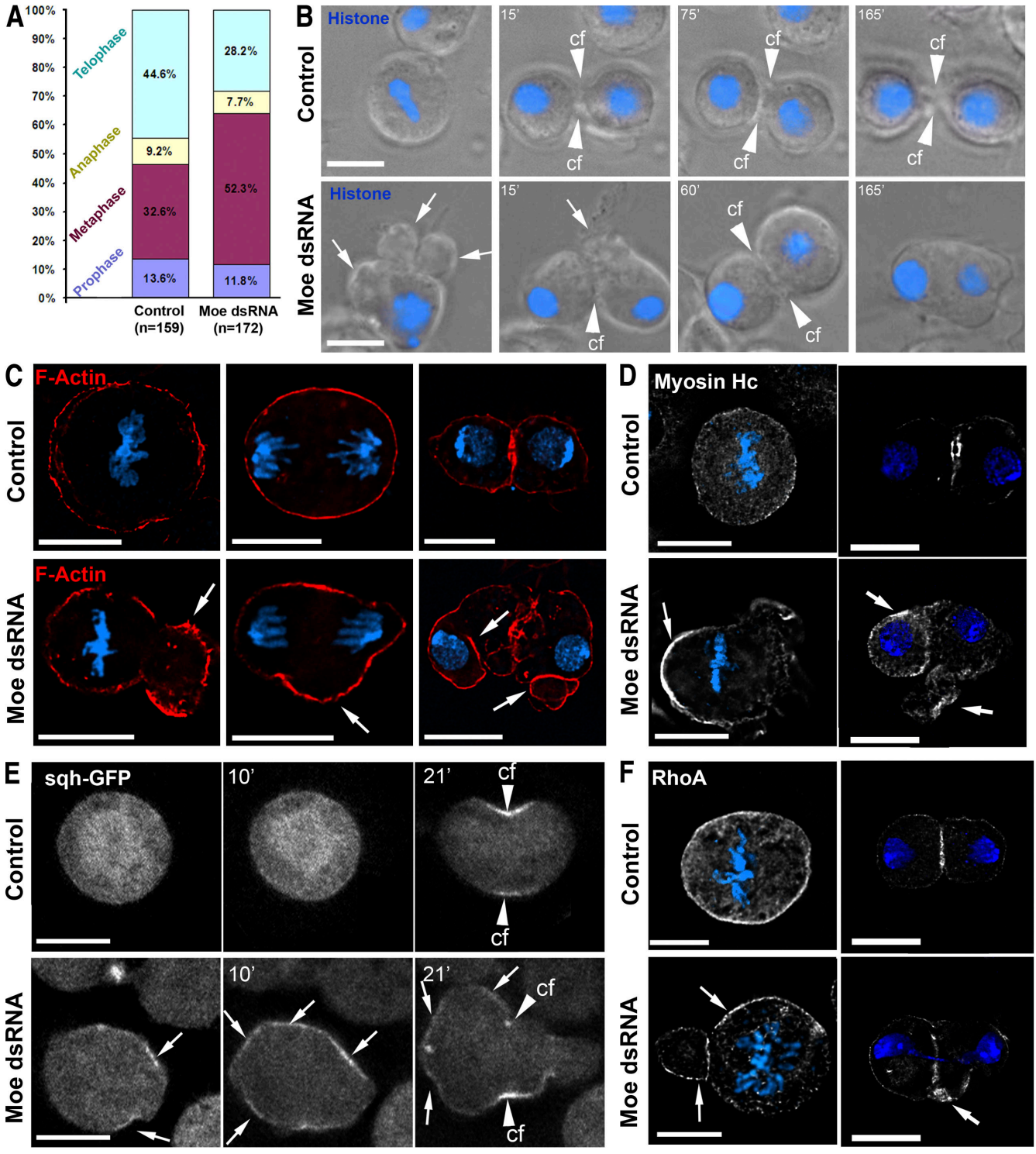

Figure 1. **Moesin controls cortex organization and contractility throughout mitosis.** (A) Proportion of mitotic cells present in the respective steps of cell division, as deduced from fixed sample examination. Inactivation of moesin led to an increased proportion of cells in metaphase over the total number of mitotic cells. This increased proportion of metaphase indicates a delayed anaphase onset, which is also apparent in most time lapses. (B) Time-lapse frames of histone H2B–GFP (blue) S2 cells in control (top) or after moesin depletion (bottom) showing abnormal cortical protrusions (arrows) from pro/metaphase to ana/telophase. In this peculiar case, there was an eventual regression of the cytokinesis furrow even though the metaphase duration was not affected. cf, cleavage furrow. (C) F-actin (red) accumulated in ectopic cell bulges (arrows) in moesin-depleted cells throughout mitosis. DNA is in blue. (D) Consequences of moesin depletion on the distribution of myosin II heavy chain in metaphase and telophase. Myosin II heavy chain was irregularly localized (arrows) in the absence of moesin. (E) Actomyosin contractions were monitored in S2 cells expressing Sqh-GFP. Moesin depletion led to the chaotic distribution of contractile myosin (arrows) and contractions. (F) Consequences of moesin depletion on the distribution of active RhoA. RhoA was irregularly localized (arrows) in the absence of moesin. Bars, 10 μm.

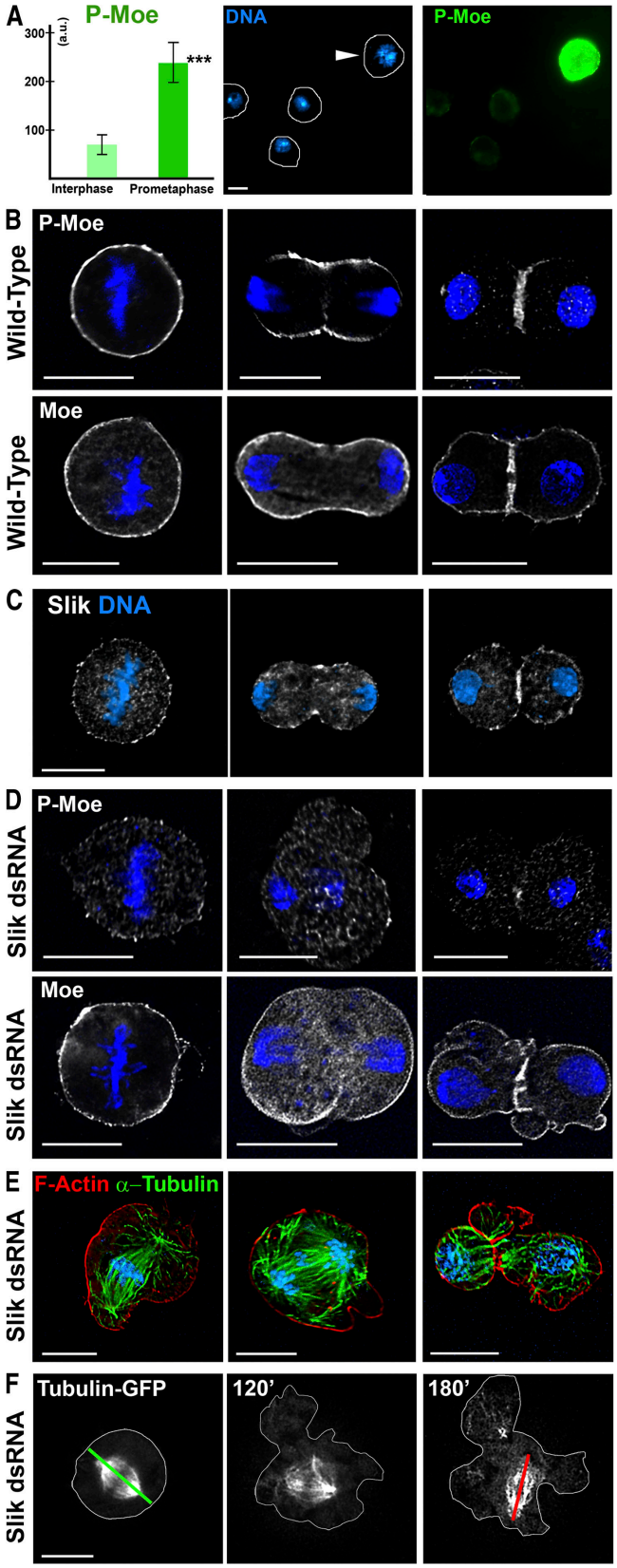

Figure 2. **The Slik kinase controls mitotic moesin function through regulation of its phosphorylation.** (A) Relative levels of p-moesin (green) in prometaphase (arrowhead) and interphase cells. Error bars represent SD. ***, $P < 0.005$. (B and D) Distribution of total moesin or p-moesin during mitosis in control (B) or Slik-depleted cells (D). (C) Cells were immunolabeled to detect the Slik protein kinase, and DNA was counterstained with DAPI (blue). (E) Defects in cell shape and microtubule organization resulting from Slik depletion. α-Tubulin, green; F-actin, red; DNA, blue. Binucleated cells were observed in 5% of Slik-depleted cells ($n = 500$). (F) Time-lapse sequences of α-tubulin–GFP cells treated by Slik dsRNA. The red lines show maximal deviations of the spindle orientation from its initial position (green lines). Bars, 10 μm.

moesin-like instability of the F-actin cortex during mitosis (Figs. 2, E and F; and S2). We observed transient cytoplasmic blebs at an erratic location of the mitotic cortex in living cells (Fig. 2 F and Video 5, available at http://www.jcb.org/cgi/content/full/jcb.200709161/DC1) as well as prominent actin-rich cortical deformations in fixed samples (Fig. 2 E). Collectively, our data show that Slik-dependent phosphorylation of moesin at T559 directs moesin activation and function during mitosis.

Absence of moesin or alteration of its activation disrupts spindle organization

The alteration of moesin activity also affected organization and stable positioning of microtubule components of the mitotic spindle from metaphase to ana/telophase. Cortical deformations were frequently associated with abnormally long astral microtubules, as observed both in fixed and living cells (Fig. 3, A and C). These data suggest that astrals might influence contractility of the cortex or, alternatively, keep growing until they meet the deformed cell cortex. In addition, the distance between the two metaphase centrosomes was significantly reduced, leading to a smaller spindle length (Figs. 3, A and B; and S2 A). These abnormal spindles were also often asymmetrical, with one of the two asters clearly more prominent than the other (Fig. 3, A and B). Although the center of the metaphase spindle was always close to the geometric center in wild type, spindles were off center in 90% of moesin-depleted cells (Fig. 3, A and B). Live imaging further revealed a continuous variation of the spindle orientation in the absence of moesin. It started during the elongated metaphase and occurred until telophase (Fig. 3 C, Fig. 4 B, and Videos 6 and 7, available at http://www.jcb.org/cgi/content/full/jcb.200709161/DC1). This instability in spindle positioning appeared unlikely to only result from a general relaxation of physical constraints (Fig. S2). It presumably involved unregulated actin-mediated contractility because it was suppressed by simultaneous treatment with RhoA-dsRNA or an F-actin–inhibiting drug (Figs. 3 C and S2 and Video 8). Finally, we observed that the absence of Slik activity mimicked the effects of moesin loss of function on the organization of the mitotic spindle. Slik depletion led to abnormal astral microtubules, spindle off-centering, as well as to destabilization of the spindle orientation from an elongated metaphase to ana/telophase (Figs. 2 F and S2 C). Therefore, these data show that Slik-mediated activation of moesin at the mitotic cortex is required for proper organization of the mitotic spindle.

We then analyzed whether modifications of the ratio between phosphorylated versus nonphosphorylated pools of the moesin protein could influence organization of the cortex and/or of the microtubule spindle. Expression of the nonphosphorylatable moesin mutant form moesin-T559A (that remained significantly associated with the cortex) caused a range of defects similar to the loss of moesin function, albeit generally less

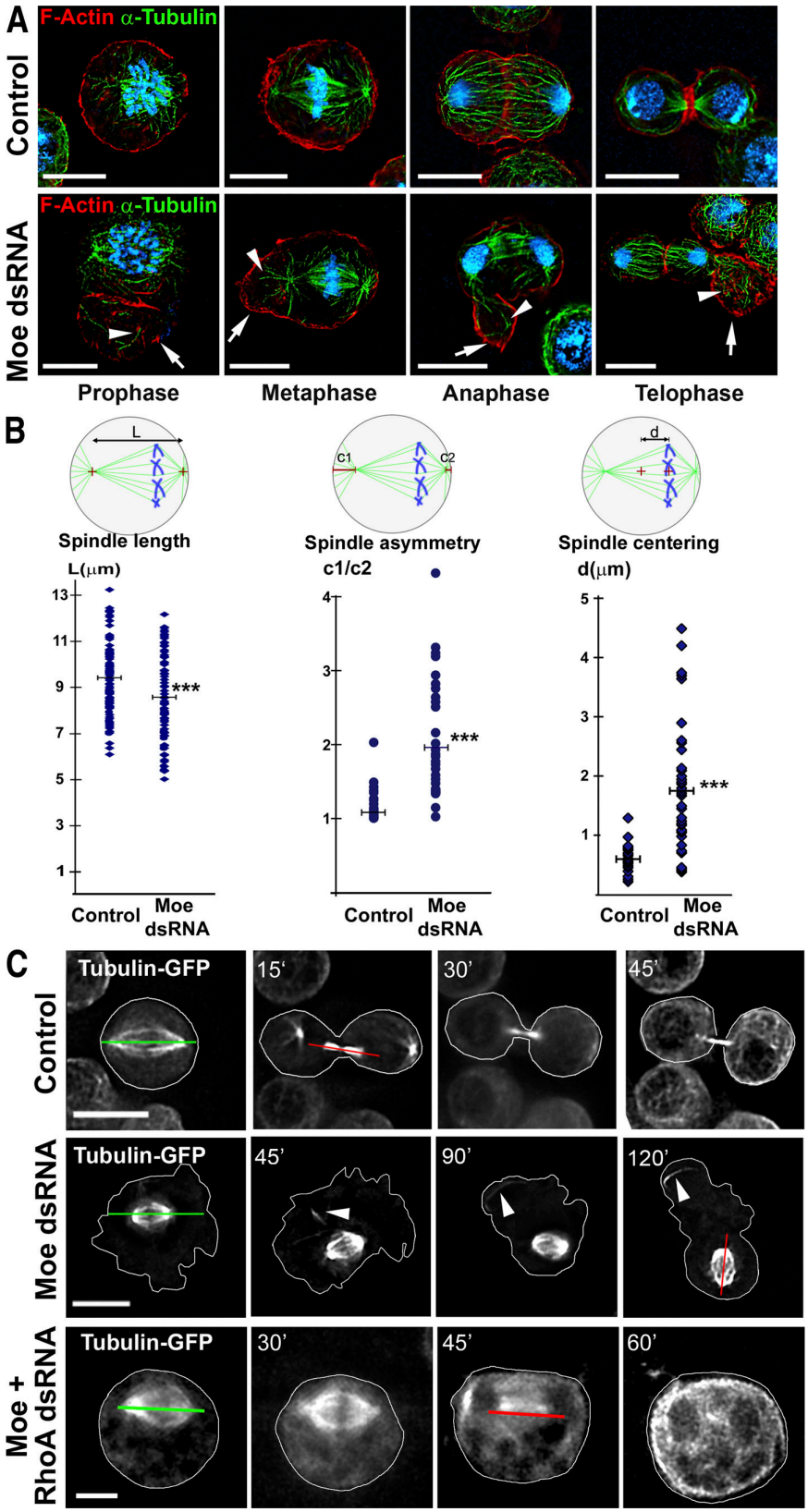

Figure 3. **Moesin inactivation impairs mitotic spindle organization and positioning.** (A) In the absence of moesin, abnormally long astral microtubules (arrowheads) contact the cortex at locations of actin-rich cell deformations (arrows). α-Tubulin, green; actin, red; DNA, blue. (B) Quantification of spindle defects in metaphase cells. L, mitotic spindle length (n = 100); c1/c2, ratio between distances of the centrosomes to their respective polar cortex (n = 25); d, distance between the geometrical center of the cell and the center of the spindle (n = 25). Each blue dot represents the calculated value for one cell. Horizontal bars represent the mean value of these data. ***, $P < 0.005$. (C) Time-lapse frames of S2 cells expressing α-tubulin–GFP treated with the indicated dsRNA. Arrowheads indicate astral microtubules associated with cortex bulges. The red lines show maximal deviations of the spindle orientation from its initial position (green lines). Bars, 10 μm.

pronounced. They included cortical instability after anaphase onset (Fig. 4, A and B) as well as enlarged cell volume in prometaphase (Fig. S2). In addition, moesin-T559A expression led to smaller spindles, which displayed unstable orientation from metaphase to ana/telophase (Fig. 4, A and B). In contrast, expression of its phosphomimetic counterpart (moesin-T559D) did not cause instability in spindle orientation, albeit spindles were also reduced in size (Figs. 4 and S2). Moesin-T559D did

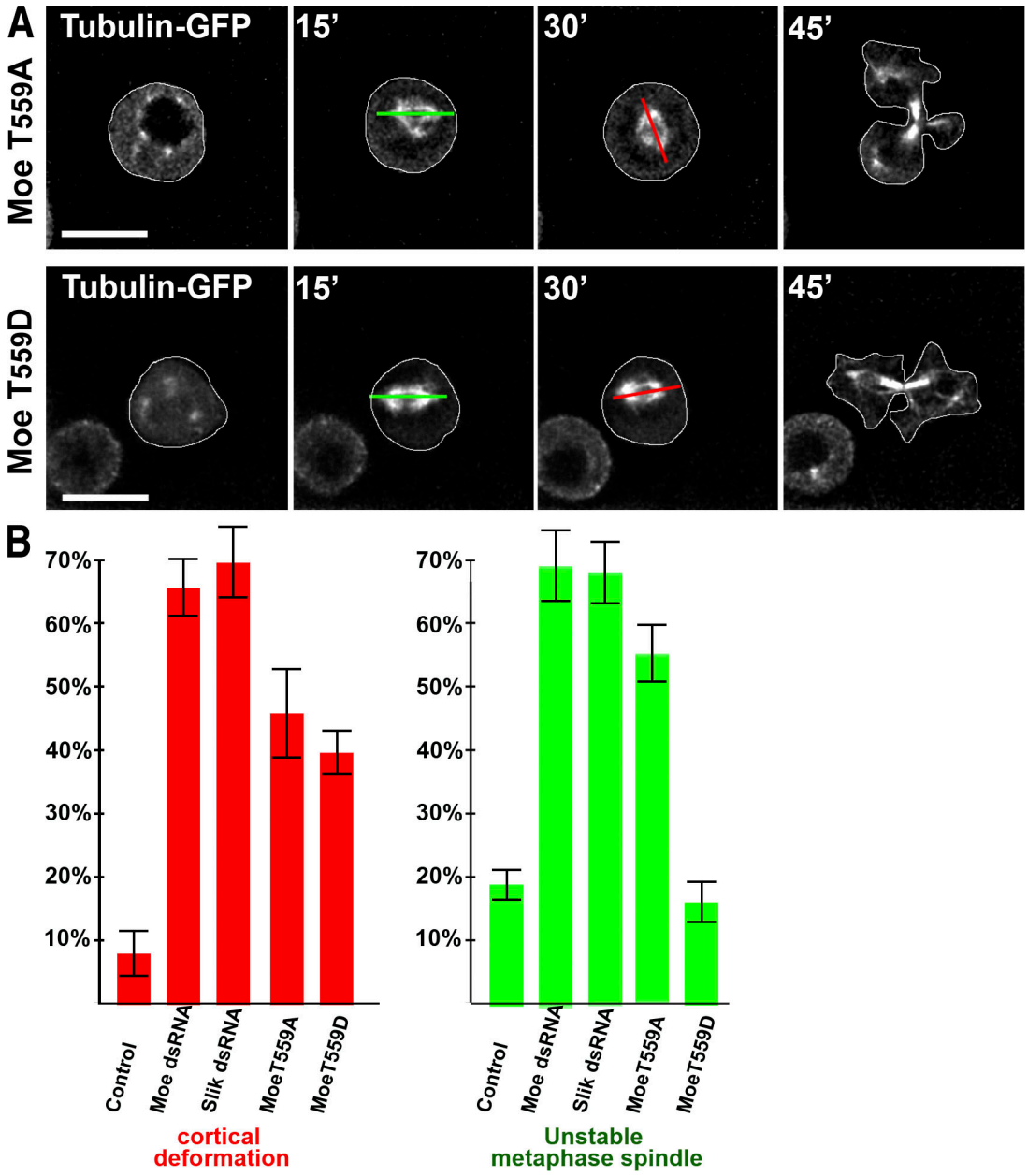

Figure 4. **Unregulated moesin phosphorylation affects organization of the cell cortex and microtubule spindle.** (A) Selected frames of dividing α-tubulin–GFP cells expressing moesin-T559A or -T559D. The red lines show maximal deviations of the spindle orientation from its initial position (green lines). (B) Relative proportions of mitotic cells displaying cortical defects (left) and destabilization of the microtubule orientation (right) after depletion in moesin or Slik and after expression of the moesin-T559A or -T559D phosphomutant moesin forms. Error bars represent SD. Bars, 10 μm.

not alter the volume of mitotic cells in prophase or metaphase but altered equatorial contraction in ana/telophase (Figs. 4 and S2). Collectively, these data bring additional support to the conclusion that the tight spatiotemporal control of moesin phosphorylation is important for normal spindle organization and mitotic cell shape.

Conclusion

Our results indicate that spatiotemporal regulation of moesin by the Slik kinase contributes to organization of the actomyosin cortex during mitosis to account for the stereotyped cell shape transformations that occur throughout cell division. In addition, our data suggest that homogenous distribution of activated moesin at the metaphase cortex is important for the proper positioning of the spindle. This model predicts that uneven ERM phosphorylation in metaphase could influence spindle orientation, a hypothesis consistent with the recent finding that extracellular matrix can guide orientation of the spindle, correlating with restricted localization of activated ERM at the cell cortex (Thery et al., 2005). Finally, activated moesin might directly or indirectly affect additional aspects of cell division because the absence of moesin or Slik lead to abnormal microtubule spindles with an asymmetrical organization, a smaller length, and delayed anaphase onset. It is possible that these spindle defects

contribute to extend the metaphase stage (e.g., through activation of mitotic checkpoints).

Thus, these results shed new light on the cross talk that occurs between microtubules and the cell cortex during mitosis. The importance of ERM proteins for normal mitosis may be relevant to human cancers that involve deregulated ERM activity (Yu et al., 2004).

Materials and methods

Fly stocks

Wild-type flies were from a w^{118} stock. We used the strains *y,w,Moe*^{PL106}*/FM7kr-Gal4,UAS-GFP*; *Moe*^{67}*/FM7kr-Gal4,UAS-GFP*; *Moe*^{404}*/FM7kr-Gal4,UAS-GFP*; *Slik*^{KG04837}*/CyO*, UAS-PblΔDH/CyO, UAS-dsRNA *Moe*/CyO, and MS1096-Gal4/FM7. To define the spermatid phenotype of cytokinesis in moesin and Slik mutants, late larval or early pupal testes were examined in living squashed preparations by phase-contrast microscopy according to Giansanti et al. (2004).

Genetic interactions in wings

UAS-PblΔDH and/or UAS-dsRNA moesin were driven at 18°C by the dorsal wing–specific driver MS1096. Quantification of the MWH (multiwing hairs) phenotype and cytokinesis defects was performed in the third posterior cell compartment under the posterior cross vein as described previously (Echard and O'Farrell, 2003).

Cell culture and dsRNA treatment

Drosophila S2 cells were grown in FCS-supplemented Schneider's medium (Invitrogen). dsRNAs were produced and used as previously described (Echard et al., 2004). For moesin and Slik extinction, we used at least two nonoverlapping regions to rule out off-target effects. Moesin-T559A and -T559D (Polesello et al., 2002) were subcloned into pAc5.1. For immunofluorescence analysis, cells were cultured for 10 min on glass coverslips coated with 10 µg concanavalin A (Sigma-Aldrich), fixed in 4% formaldehyde (except for p-moesin and RhoA staining, in which the cells were fixed in 10% TCA), and processed for immunostaining (Echard et al., 2004). We used antimoesin (Polesello et al., 2002) at 1:5,000, anti–p-moesin (Karagiosis and Ready, 2004) at 1:500, anti–α-tubulin (Sigma-Aldrich) at 1:200, anti-RhoA (Magie et al., 2002) at 1:50, anti–myosin-Hc (obtained from R. Karess, Centre National de la Recherche Scientifique/Centre de Genetique Moleculaire, Gif-Sur-Yvette, France) at 1:200, and anti-Slik (Hipfner et al., 2004) at 1:100. AlexaFluor488, AlexaFluor546, and Cy5-conjugated secondary antibodies (Invitrogen) were used at 1:500. Texas red-X phalloidin (Invitrogen) was used at 1:200 for F-actin staining. The primer sequences used are as follows: Moe_1 (forward, AACGCCAAGGATGAGGAGAC; reverse, ACGCTTTGTGTTGCCCTTAC), Moe_2 (forward, AGGAGCTGATCCAGGACATTACA; reverse, CTGCTGTTTGGCATTCTTCTC), Moe_3 (forward, AGACGCTTTGTCTCCTCATCC; reverse, GAAAAGAAGCAGCAGGAGTACG), Slik_1 (forward, ACTTTGTCAAAAAGGGTAAGGC; reverse, ACCTCACTTTCATCCAGTTTGC), Slik_2 (forward, TAGGACAGCAGCAATGAGCTGG; reverse, TTCACGTAGCTCCTGCTTACGG), and RhoA (forward, ATCAAGAACAACCAGAACATCG; reverse, TTTGTTTTGTGTTTAGTTCGGC).

Imaging of fixed samples and time-lapse recording

Images of fixed cells mounted in Vectashield (Vector Laboratories) were acquired using a microscope (DMIRE2; Leica) with voxels collected at 104-nm lateral and 200-nm axial intervals using a stage (PIFOC piezo; Physik Instrumente) and a cooled camera (MicroMax-1300Y-HS; Princeton Instruments). Deconvolution was performed using Huygens software (Scientific Volume Imaging) on a Silicon Graphics Origin computer.

Video microscopy (Eggert et al., 2006; Hickson et al., 2006) was performed using stable cell lines expressing histone-GFP, tubulin-GFP, or Spaghetti-squash-GFP plated directly on 96-well glass-bottom plates (Greiner) at 25°C and imaged with a microscope (DMIRBE; Leica) and a MicroMax cooled CCD camera controlled by MetaMorph 6.1 software (MDS Analytical Technologies). Z series of five 1-µm sections were used to generate maximum intensity projections, and images were processed using Huygens software. All images were prepared for publication using Photoshop software (Adobe).

Online supplemental material

Fig. S1 shows that the reduction of moesin activity led to mild cytokinesis defects in vivo and in S2 cultured cells. Fig. S2 shows quantification of the mitotic defects observed in S2 cells after moesin depletion and other treatments. Videos 1 and 2 show phase-contrast and histone-GFP in control S2 cells (Video 1) and in moesin-depleted S2 cells (6 d of dsRNA treatment; Video 2). Videos 3 and 4 show Sqh-GFP in control S2 cells (Video 3) and in moesin-depleted S2 cells (6 d of dsRNA treatment; Video 4). Videos 5 and 6 show tubulin-GFP in Slik-depleted S2 cells (6 d of dsRNA treatment; Video 5) and in control S2 cells (Video 6). Videos 7 and 8 show tubulin-GFP in moesin-depleted S2 cells (6 d of dsRNA treatment; Video 7) and in moesin + RhoA double-depleted S2 cells (moesin, 6 d of dsRNA treatment; RhoA, 3 d of dsRNA treatment; Video 8). Online supplemental material is available at http://www.jcb.org/cgi/content/full/jcb.200709161/DC1.

We thank B. Goud (in whose laboratory I. Kouranti and A. Echard have done this work), B. Baum for sharing unpublished data, D. Ready, S. Cohen, R. Karess, the Bloomington Stock Center and Developmental Studies Hybridoma Bank for antibodies and materials, and P. Valenti and C. Polesello for their help. We thank S. Tournier and Y. Gachet for sharing ideas on the project, and J.C. Labbé, P. O'Farrell, and M. Arpin for critical reading of the manuscript.

This work was supported by the Ministère de la Recherche et de la Technologie (grant to I. Kouranti), the American Heart Association Western States Affiliate (grant to E.S. Glusman), National Institutes of Health (grant 1R01GM62276 to M.T. Fuller), the Association pour la Recherche sur le Cancer (no. 3832; grant to F. Payre), the Fondation pour la Recherche Médicale (fellowships to S. Carreno and programme équipe 2005), Agence Nationale de Recherche (grant JC07-188506 to A. Echard), and by a Career Development Award (grant HFSP CDA-2006 to S. Carreno).

Submitted: 25 September 2007
Accepted: 24 January 2008

Note added in proof. A recent study from Kunda et al. (2008) reports a similar role of dmoesin and its regulator Slik in the cortical organization of another *Drosophila* cell line during division.

References

Bement, W.M., H.A. Benink, and G. von Dassow. 2005. A microtubule-dependent zone of active RhoA during cleavage plane specification. *J. Cell Biol.* 170:91–101.

Bettencourt-Dias, M., R. Giet, R. Sinka, A. Mazumdar, W.G. Lock, F. Balloux, P.J. Zafiropoulos, S. Yamaguchi, S. Winter, R.W. Carthew, et al. 2004. Genome-wide survey of protein kinases required for cell cycle progression. *Nature.* 432:980–987.

Bjorklund, M., M. Taipale, M. Varjosalo, J. Saharinen, J. Lahdenpera, and J. Taipale. 2006. Identification of pathways regulating cell size and cell-cycle progression by RNAi. *Nature.* 439:1009–1013.

Bretscher, A., K. Edwards, and R.G. Fehon. 2002. ERM proteins and merlin: integrators at the cell cortex. *Nat. Rev. Mol. Cell Biol.* 3:586–599.

Canman, J.C., L.A. Cameron, P.S. Maddox, A. Straight, J.S. Tirnauer, T.J. Mitchison, G. Fang, T.M. Kapoor, and E.D. Salmon. 2003. Determining the position of the cell division plane. *Nature.* 424:1074–1078.

Charras, G.T., J.C. Yarrow, M.A. Horton, L. Mahadevan, and T.J. Mitchison. 2005. Non-equilibration of hydrostatic pressure in blebbing cells. *Nature.* 435:365–369.

Chorna-Ornan, I., V. Tzarfaty, G. Ankri-Eliahoo, T. Joel-Almagor, N.E. Meyer, A. Huber, F. Payre, and B. Minke. 2005. Light-regulated interaction of Dmoesin with TRP and TRPL channels is required for maintenance of photoreceptors. *J. Cell Biol.* 171:143–152.

Coscoy, S., F. Waharte, A. Gautreau, M. Martin, D. Louvard, P. Mangeat, M. Arpin, and F. Amblard. 2002. Molecular analysis of microscopic ezrin dynamics by two-photon FRAP. *Proc. Natl. Acad. Sci. USA.* 99:12813–12818.

Echard, A., and P.H. O'Farrell. 2003. The degradation of two mitotic cyclins contributes to the timing of cytokinesis. *Curr. Biol.* 13:373–383.

Echard, A., G.R. Hickson, E. Foley, and P.H. O'Farrell. 2004. Terminal cytokinesis events uncovered after an RNAi screen. *Curr. Biol.* 14:1685–1693.

Eggert, U.S., A.A. Kiger, C. Richter, Z.E. Perlman, N. Perrimon, T.J. Mitchison, and C.M. Field. 2004. Parallel chemical genetic and genome-wide RNAi screens identify cytokinesis inhibitors and targets. *PLoS Biol.* 2:e379.

Eggert, U.S., T.J. Mitchison, and C.M. Field. 2006. Animal cytokinesis: from parts list to mechanisms. *Annu. Rev. Biochem.* 75:543–566.

Giansanti, M.G., R.M. Farkas, S. Bonaccorsi, D.L. Lindsley, B.T. Wakimoto, M.T. Fuller, and M. Gatti. 2004. Genetic dissection of meiotic cytokinesis in *Drosophila* males. *Mol. Biol. Cell.* 15:2509–2522.

Glotzer, M. 2005. The molecular requirements for cytokinesis. *Science.* 307:1735–1739.

Hickson, G.R., A. Echard, and P.H. O'Farrell. 2006. Rho-kinase controls cell shape changes during cytokinesis. *Curr. Biol.* 16:359–370.

Hipfner, D.R., N. Keller, and S.M. Cohen. 2004. Slik Sterile-20 kinase regulates Moesin activity to promote epithelial integrity during tissue growth. *Genes Dev.* 18:2243–2248.

Hughes, S.C., and R.G. Fehon. 2006. Phosphorylation and activity of the tumor suppressor Merlin and the ERM protein Moesin are coordinately regulated by the Slik kinase. *J. Cell Biol.* 175:305–313.

Hughes, S.C., and R.G. Fehon. 2007. Understanding ERM proteins–the awesome power of genetics finally brought to bear. *Curr. Opin. Cell Biol.* 19:51–56.

Jankovics, F., R. Sinka, T. Lukacsovich, and M. Erdelyi. 2002. MOESIN crosslinks actin and cell membrane in *Drosophila* oocytes and is required for OSKAR anchoring. *Curr. Biol.* 12:2060–2065.

Karagiosis, S.A., and D.F. Ready. 2004. Moesin contributes an essential structural role in *Drosophila* photoreceptor morphogenesis. *Development.* 131:725–732.

Kunda, P., A.E. Pelling, T. Liu , and B. Baum. 2008. Moesin controls cortical rigidity, cell rounding, and spindle morphogenesis during mitosis. *Curr. Biol.* 18:91–101.

Maddox, A.S., and K. Burridge. 2003. RhoA is required for cortical retraction and rigidity during mitotic cell rounding. *J. Cell Biol.* 160:255–265.

Magie, C.R., D. Pinto-Santini, and S.M. Parkhurst. 2002. Rho1 interacts with p120ctn and alpha-catenin, and regulates cadherin-based adherens junction components in *Drosophila*. *Development.* 129:3771–3782.

Matzke, R., K. Jacobson, and M. Radmacher. 2001. Direct, high-resolution measurement of furrow stiffening during division of adherent cells. *Nat. Cell Biol.* 3:607–610.

Pilot, F., J.M. Philippe, C. Lemmers, and T. Lecuit. 2006. Spatial control of actin organization at adherens junctions by a synaptotagmin-like protein Btsz. *Nature.* 442:580–584.

Polesello, C., I. Delon, P. Valenti, P. Ferrer, and F. Payre. 2002. Dmoesin controls actin-based cell shape and polarity during *Drosophila melanogaster* oogenesis. *Nat. Cell Biol.* 4:782–789.

Sato, N., S. Yonemura, T. Obinata, S. Tsukita, and S. Tsukita. 1991. Radixin, a barbed end-capping actin-modulating protein, is concentrated at the cleavage furrow during cytokinesis. *J. Cell Biol.* 113:321–330.

Speck, O., S.C. Hughes, N.K. Noren, R.M. Kulikauskas, and R.G. Fehon. 2003. Moesin functions antagonistically to the Rho pathway to maintain epithelial integrity. *Nature.* 421:83–87.

Strickland, L.I., E.J. Donnelly, and D.R. Burgess. 2005a. Induction of cytokinesis is independent of precisely regulated microtubule dynamics. *Mol. Biol. Cell.* 16:4485–4494.

Strickland, L.I., Y. Wen, G.G. Gundersen, and D.R. Burgess. 2005b. Interaction between EB1 and p150glued is required for anaphase astral microtubule elongation and stimulation of cytokinesis. *Curr. Biol.* 15:2249–2255.

Thery, M., V. Racine, A. Pepin, M. Piel, Y. Chen, J.B. Sibarita, and M. Bornens. 2005. The extracellular matrix guides the orientation of the cell division axis. *Nat. Cell Biol.* 7:947–953.

Verdier, V., J.E. Johndrow, M. Betson, G.C. Chen, D.A. Hughes, S.M. Parkhurst, and J. Settleman. 2006. *Drosophila* Rho-kinase (DRok) is required for tissue morphogenesis in diverse compartments of the egg chamber during oogenesis. *Dev. Biol.* 297:417–432.

Yu, Y., J. Khan, C. Khanna, L. Helman, P.S. Meltzer, and G. Merlino. 2004. Expression profiling identifies the cytoskeletal organizer ezrin and the developmental homeoprotein Six-1 as key metastatic regulators. *Nat. Med.* 10:175–181.